Science Background for the Reprocessing and Goddard Satellite-based Surface Turbulent Fluxes (GSSTF3) Dataset for Global Water and Energy Cycle Research

Version 1.0

Release Date: May 29, 2012
Updated Date: November 19, 2012

Goddard Earth Sciences Data and Information Services Center (GES DISC)
http://disc.gsfc.nasa.gov
NASA Goddard Space Flight Center
Code 610.2
Greenbelt, MD 20771 USA

Science Background for the Reprocessing and Goddard Satellite-based Surface Turbulent Fluxes (GSSTF3) Dataset for Global Water and Energy Cycle Research

The global water cycle's provision of water to terrestrial storage, reservoirs, and rivers rests upon the global excess of evaporation to precipitation over the oceans. Variations in the magnitude of this ocean evaporation excess will ultimately lead to variations in the amount of freshwater that is transported (by the atmosphere) and precipitated over continental regions. The air-sea fluxes of momentum, radiation, and freshwater (precipitation – evaporation) play a very essential role in a wide variety of atmospheric and oceanic problems (e.g., oceanic evaporation contributes to the net fresh water input to the oceans and drives the upper ocean density structure and consequently the circulation of the oceans). Information on these fluxes is crucial in understanding the interactions between the atmosphere and oceans, the global energy and water cycle variability, as well as in improving model simulations of climate variations.

The GSSTF3 (Version 3) dataset is an upgraded and improved version with a finer spatial resolution (0.25° x 0.25°) compared to the preceding GSSTF2c (1° x 1°) dataset released in October 2011. Similar to GSSTF2c, the brightness temperature (Tb) of the Special Sensor Microwave Imager (SSM/I) [on board of a series of Defense Meteorological Satellite Program (DMSP) satellites] applied for retrieving the surface specific humidity (Qair) has been corrected by removing its dependence from the Earth incidence angle (EIA) drifting (Hilburn and Shie 2011). In this new GSSTF3 production, we have adopted an updated and improved algorithm for retrieving Qair directly from Tb (Bentamy et al. 2003). In the preceding GSSTF products, e.g., the currently distributed GSSTF2c, Qair was retrieved involving a two-step approach: the bottom-layer (the lowest atmospheric 500 meter layer) precipitable water (WB) was first obtained from Tb (Schulz et al. 1993), and then Qair was retrieved based on WB and the total precipitable water (W) using an Empirical Orthogonal Function (EOF) method (Chou et al. 1995; 1997). GSSTF3 has been found possessing a further reduced temporal trend in the retrieved Qair, and latent heat flux (E or LHF) subsequently, than those of GSSTF2c.

Document maintained by *GES DISC Personnel*

Prepared by: Chung-Lin Shie (UMBC/JCET, Code 612.0)

Edited and approved by: Andrey K. Savtchenko

Dataset Provider: Goddard Earth Sciences Data and Information Services Center
Dataset Provider Address: Code 610.2, NASA Goddard Space Flight Center, Greenbelt Rd., Greenbelt, MD 20771, USA

Table of Contents

1 Introduction

This document provides basic information for using Goddard Satellite-based Surface Turbulent Fluxes Version 3 (a.k.a. GSSTF3) Dataset products.

The GSSTF3 (July 1987-December 2008) consists of products generated for the focus on Global Water and Energy Cycle Research. The global water cycle's provision of water to terrestrial storage, reservoirs, and rivers rests upon the global excess of evaporation to precipitation over the oceans. Variations in the magnitude of this ocean evaporation excess will ultimately lead to variations in the amount of freshwater that is transported (by the atmosphere) and precipitated over continental regions. The air-sea fluxes of momentum, radiation, and freshwater (precipitation – evaporation) play a very essential role in a wide variety of atmospheric and oceanic problems (e.g., oceanic evaporation contributes to the net fresh water input to the oceans and drives the upper ocean density structure and consequently the circulation of the oceans). Information on these fluxes is crucial in understanding the interactions between the atmosphere and oceans, the global energy and water cycle variability, as well as in improving model simulations of climate variations.

2 Overview and Background

2.1 Product/Algorithm Objectives

The recently distributed GSSTF datasets, i.e., GSSTF2c (July 1987-December 2008) and the recently retired GSSTF2b (July 1987-December 2008), have been widely used by scientific communities for global energy and water cycle research, and regional and short period data analysis since their official releases in October 2011 and October 2010, respectively, via NASA GES DISC. According to the automatically updated monthly records performed by the Earth Science Data and Information System (ESDIS) Metrics System (EMS), there have been 252,659 numbers of product (granules) and 376.8 GB data volume delivered to 351 distinct users up to July 2012.

The objective of this project is to continually produce a uniform and improved dataset of sea surface turbulent fluxes (i.e., latent heat flux, sensible heat flux and wind stress) derived from remote sensing data (SSM/I) and reanalysis (NCEP) that would continue to be useful for global energy and water flux research and applications. We are looking forward to serving the scientific communities with one more useful dataset in GSSTF3.

2.2 Historic Perspective

Accurate sea surface fluxes measurements are crucial to understanding the global water and energy cycles. The oceanic evaporation that is a major component of the global oceanic fresh water flux is particularly useful to predicting oceanic circulation and transport. The GSSTF products distributed so far, i.e., from GSSTF2 (Chou et al. 2001; Chou et al. 2003), GSSTF2b (Shie et al. 2010a,b; Shie 2010a,b; Shie et al. 2009) to GSSTF2c (Shie et al. 2011; Shie 2011), have been widely used by scientific communities. Our records (based mainly on website online retrievals plus some personal communications) indicate that numerous individuals or groups have used the GSSTF datasets for scientific research. There have been 280 GSSTF-related research studies published either in peer-reviewed journals (i.e., 125) or non-peer reviewed publications such as conference presentations/papers, book chapters, technical reports, dissertations or theses, etc. (i.e., 155) by October 2012. The users ranging from government agencies, universities, institutes to private scientific companies from various countries have performed diversified scientific projects.

The preceding GSSTF2b possessed a temporal trend in the globally averaged latent heat flux, E or LHF, particularly post 2000, which was mainly due to the artificial trends of the SSM/I Tb (Shie 2010a,b) that were subsequently attributed by Hilburn and Shie (2011) primarily to the drift in EIA associated with the SSM/I sensors on the DMSP satellites. An algorithm that would properly remove the SSM/I Tb dependence from the EIA drifting was thus successfully developed by Hilburn and Shie (2011). The GSSTF2c dataset (Shie et al. 2011) was subsequently produced using the corrected SSM/I Tb through application of the algorithm (Hilburn and Shie 2011). As a result, WB, Qair and E of GSSTF2c were found genuinely improved, particularly in the trends post 2000 (Shie and Hilburn 2011; Shie 2011). In this GSSTF3 production, we have further adopted an updated and improved algorithm for retrieving Qair directly from Tb (Bentamy et al. 2003), instead of using the two-step approach in producing the rest/preceding GSSTF datasets, e.g., the currently distributed GSSTF2c and recently retired GSSTF2b. In the two-way approach, the bottom-layer precipitable water, WB, was first obtained from Tb (Schulz et al. 1993) followed by retrieving Qair based on WB and W using an EOF method (Chou et al. 1995; 1997). As such, the "intermediate" field, WB, used to be produced in GSSTF2c and GSSTF2b is no longer created in GSSTF3. Consequently, GSSTF3 has been found with a further reduced trend in the retrieved globally averaged Qair and E as compared to GSSTF2c.

The GSSTF3 production, similar to the GSSTF2c production, also uses the input datasets such as the SSM/I V6 surface/10-m wind speeds (U), as well as the sea surface temperature (SST), 2-m air temperature (Tair_2m), and sea level pressure (Psea_level) of the NCEP/DOE Reanalysis-2 (R2), along with the Cross-Calibrated Multi-Platform (CCMP) ocean surface wind vector product (Atlas et al., 2009). However, note that the SSM/I total precipitable water, W, is no longer used in the GSSTF3 production, but still distributed as one of the output data for providing extra information. GSSTF3 has a finer spatial resolution (0.25° x 0.25°) than the preceding GSSTF2c (1° x 1°). Additionally, Digital Object Identifiers (DOI) is newly registered for each data product of GSSTF3.

2.3 Data Product Characteristics

Similar to the preceding GSSTF2c, GSSTF3 (July 1987-December 2008) possesses one “Combined” dataset based on one set of combination of individual satellite products. The GSSTF3 data are stored in HDF-EOS5 files.

The GSSTF3 daily fluxes have first been produced for each available individual SSM/I satellite tapes, i.e., F08, F10, F11, F13, F14 and F15. Then, the Combined daily fluxes are produced by averaging (equally weighted) over available flux data/files from various satellites. These Combined daily flux data are considered as the "final" GSSTF3, and are stored, along with the individual satellite data, in this HDF-EOS5 collection. Data should be used with care and proper citations, i.e., properly indicating your applications with, e.g., "using the combined 2001 data file" or "using the 2001 F13 data file". The users may feel free to use the products of the Combined or the individual satellites with their own interests and purposes.

The MEaSUREs project at GES DISC converted all data (in binary) into HDF-EOS5 format and reorganized it into separate daily and monthly files, in a manner consistent with the ongoing Earth Observing System (EOS) missions such as Aura, Aqua, and Terra. The monthly, seasonal and yearly climatologies are also in HDSF-EOS5 format, in separate files. As such, the daily files are now easily searchable and downloadable by data day.

The essential meaning of HDF-EOS5 is that the data are now in a standard “Grid” format. The GSSTF3 seven major variables are grouped into one grid, named “SET1”, and stored in one file. Further, the “minor” variable - total precipitable water - is also grouped together with the seven major variables in the corresponding SET1 grid. Thus the grid contains 8 variables. This organization is identical for all daily and monthly files, apart from the model reanalysis. The “common”, NCEP/DOE Reanalysis II, data are stored in separate files with one Grid containing the four “common” variables. The climatologies (monthly, seasonal, and yearly) also contain the SET1 grid, but in addition are also containing the four NCEP variables in a separate grid.

The “individual tapes” representing the individual SSM/I satellites are stored in separate collections and daily files, one day per file. They contain one grid that is named on the satellite name (F08, F10, F11, F13, F14, and F15). The grid contains the eight variables (7 major + 1 minor) that go into the computation of the final eight “combined” retrieved variables.

All data within these HDF-EOS5 are easily recognizable as 1440x720 arrays, representing global map, at 0.25x0.25 deg grid cell size. The endianness of the remote storage and the users’ local machines become irrelevant. The concept of headers and offsets, typical for the binary format, disappears and all that matters are Grid and data field names that are very easy to list out using command line utilities.

This data organization results in 13 data types, with Short Names listed below. The Short Name is the first string in all filenames, and it is also stored inside the files as a global file attribute “ShortName”.

A. Daily:
There are total of six (8) daily data types.

GSSTF
GSSTF_NCEP
GSSTF_F08
GSSTF_F10
GSSTF_F11
GSSTF_F13
GSSTF_F14
GSSTF_F15

1) GSSTF
It has 1 grid, "SET1". Every grid has 8 parameters, the 7 "major" plus the "minor" total precipitable water.

2) GSSTF_NCEP
It has one grid, "NCEP", with 4 parameters. The original were the "common" binary files, that is the NCEP/DOE Reanalysis II.

3) GSSTF_Fxx
These are the individual satellites, where Fxx is one of the following, i.e., F08, F10, F11, F13, F14, and F15. The HDF-EOS5 files have only one grid, which takes the name of the individual satellite. Every grid has 8 parameters, the 7 "major" plus the "minor" total precipitable water.

B. Monthly:
There are two (2) Monthly data types in he5.
GSSTFM
GSSTFM_NCEP

1) GSSTFM
It has two (2) grids: SET1, and SET1_INT, where "INT" stands for interpolated. Each of these has 8 (eight) parameters: the 7 "major" plus the "minor" total precipitable water.

2) GSSTFM_NCEP
This is the "common" monthly NCEP/DOE Reanalysis II. It has one grid with four parameters.

C. Climatology
There are three (3) climatological data types: Monthly, Seasonal, and Yearly in HDF-EOS5:
GSSTFMC
GSSTFSC
GSSTFYC

The climatologies (monthly, seasonal, and yearly) also contain the SET1 grid, but in addition are also containing the four NCEP/DOE Reanalysis II variables in a separate grid, “NCEP”.

Summary of All Data Types:
GSSTF
GSSTF_NCEP
GSSTF_F08
GSSTF_F10

GSSTF_F11
GSSTF_F13
GSSTF_F14
GSSTF_F15
GSSTFM
GSSTFM_NCEP
GSSTFMC
GSSTFSC
GSSTFYC

The file naming convention for the non-climatological HDF-EOS5 files produced at GES DISC for the GSSTF3 project is as follows:

ShortName.vv.yyyy.mm.dd.he5

Where:

- ShortName = one of the following Data Types:
  GSSTF
  GSSTF_NCEP
  GSSTF_F08
  GSSTF_F10
  GSSTF_F11
  GSSTF_F13
  GSSTF_F14
  GSSTF_F15
  GSSTFM
  GSSTFM_NCEP
  GSSTFMC
  GSSTFSC
  GSSTFYC

- vv = 3 for this release
- yyyy = data year
- mm= data month
- dd = start date for the data
- he5 = commonly accepted extension for HDF-EOS5 files.

Filename example for the daily "combined" turbulent fluxes retrieval, for November 1, 2000:
GSSTF.**3**.2000.11.01.he5

Climatologies have slightly different file names that reflect the Month (for monthlies), the range of Months (for seasonal), and the range of Years for which the climatology is built. The yearly climatology has one file only.

Example file name for Monthly climatology for November:

GSSTFMC.3.Nov.1988_2008.he5

Example file name for seasonal climatology for September-November:

GSSTFSC.3.Sep_Nov.1988_2008.he5

Each **SET1** grid (including interpolated, SET1_INT) contains the following 8 science data fields:

data_field_short_name	Data field long name (units)
"E"	'latent heat flux' (W/m**2)
"STu"	'zonal wind stress' (N/m**2)
"STv"	'meridional wind stress' (N/m**2)
"H"	'sensible heat flux' (W/m**2)
"Qair"	'surface air (~10-m) specific humidity' (g/kg)
"U"	'10-m wind speed' (m/s)
"DQ"	'sea-air humidity difference' (g/kg)
"Tot_Precip_Water"	'total precipitable water' (g/cm**2)

Each NCEP Grid contains the following 4 data fields:

Data field short name	Data field long name (units)
"SST"	'sea surface skin temperature' (C)
"Psea_level"	'sea level pressure' (hPa)
"Tair_2m"	'2m air temperature' (C)
"Qsat"	'sea surface saturation humidity' (g/kg)

3 Physics of the Problem

The Earth's climate is characterized by a myriad of processes that couple the ocean, land, and atmosphere systems. The global water cycle's provision of water to terrestrial storage, reservoirs, and rivers rests upon the global excess of evaporation to precipitation over the oceans. Variations in the magnitude of this ocean evaporation excess will ultimately lead to variations in the amount of freshwater that is transported (by the atmosphere) and precipitated over continental regions. The air-sea fluxes of momentum, radiation, and freshwater (precipitation – evaporation) play a very essential role in a wide variety of atmospheric and oceanic problems. Information on these fluxes is crucial in understanding the interactions between the atmosphere and oceans, the global energy and water cycle variability, as well as in improving model simulations of climate variations. These fluxes are thus

required for driving ocean models and validating coupled ocean–atmosphere global models. Surface measurements of these fluxes are scarce in both space and time, especially over the oceans and in remote land areas. The Comprehensive Ocean–Atmosphere Data Set (COADS) has collected the most complete surface marine observations since 1854, mainly from merchant ships (Woodruff et al. 1993). However, the air–sea fluxes and input variables based on COADS have serious spatial and temporal sampling problems plus measurement uncertainty. It is, therefore, desirable that long-term global datasets of these fluxes be derived either from satellite observations or general circulation models (GCMs). Indeed, satellite measurements nicely complement conventional data to provide or improve space/time estimates of many hydrologic parameters. Several efforts have been made to prepare datasets of ocean surface turbulent fluxes from satellite observations using bulk flux models. The SSM/I on board a series of DMSP satellites spacecraft has provided global radiance measurements (e.g., the brightness temperature, Tb) for sensing the atmosphere and the surface. A number of techniques have been developed to derive the turbulent fluxes using parameters such as the surface air humidity and winds inferred from the SSM/I radiances (e.g., Chou et al. 1997; Schulz et al. 1997; Kubota et al. 2002; Bentamy et al. 2003). We would like to particularly reemphasize the two important aspects/actions involving in the GSSTF3 production. The first feature (also involved in GSSTF2c) is the correction on the SSM/I Tb's by removing the associated artificial EIA drifting effect (Hilburn and Shie 2011) before applying them for the Qair retrieval. The second feature is the newly adoption of the Qair-Tb formulation (Bentamy et al. 2003) for a direct Qair retrieval using the corrected Tb's. The former has genuinely improved GSSTF2c by reducing the temporal trend of E compared to GSSTF2b, while the latter has further reduced the E trend in the thus improved GSSTF3 compared to GSSTF2c.

4 Retrieval Algorithms

4.1 Ancillary Data Requirements

Similar to the preceding GSSTF2c fluxes, the GSSTF3 fluxes are produced using the up-to-date and improved input datasets, i.e., the SSM/I V6 surface/10-m wind speeds (U), as well as the NCEP/DOE Reanalysis-2 (R2) SST, 2-m air temperature (Tair_2m), and sea level pressure (Psea_level). The corrected SSM/I Tb incorporating proper adjustment to the EIA drifts (Hilburn and Shie 2011) is used for retrieving surface air (~10m) specific humidity (Qair) (Bentamy et al. 2003). Qair and Qsat (surface saturation specific humidity based on SST), SST, Tair_2m and U are eventually applied in the GSSTF bulk flux model/algorithm to produce the three air-sea turbulent fluxes, i.e., wind stress (τ or WST), sensible heat flux (H or SHF), and latent heat flux (E or LHF). Moreover, the CCMP ocean surface wind vector is used to partition τ into the respective wind stress vectors, i.e., STu and STv.

4.2 Calibration and Validation

The SSM/I V4 surface wind speeds that carried a linear trend of 6% increase in a 13.5-year period (Xing 2006) were used for producing the earlier version GSSTF2. The SSM/I V6 product in which the spurious wind speed trends were removed by Remote Sensing Systems (RSS) was used for producing GSSTF2c (Shie et al. 2011; Shie 2011) and GSSTF2b (Shie et al. 2010a,b; Shie 2010a,b; Shie et al. 2009), which is now also applied for the GSSTF3 production. Shie et al. (2009; 2010a) showed a generally consistent improvement in the surface wind speed from SSM/I V4 to V6 by comparing the daily V6 and V4 (combined F13 and F14) surface wind speeds with in situ observed wind speeds from the five field experiments in 1999, i.e., Kwajalein Experiment (KWAJEX), the Joint Air–Sea Monsoon Interaction Experiment (JASMINE), the buoy service in the North Pacific (MOORINGS), the Nauru'99 (NAURU99), and the Pan–American Climate Study in the eastern Pacific during 1999 (PACSF99). Statistics showed a commonly reduced root-mean-square and bias, and increased correlation coefficient from V4 to V6 in four of the five experiments, except for NAURU99. As a result, GSSTF2b generally agreed better with the five 1999 ship measurements than its counterpart GSSTF2 did in all three flux components – latent heat flux E/LHF, sensible heat flux H/SHF, and wind stress WST (Shie 2010a; Shie et al. 2010a). Brunke et al. (2011) also found that GSSTF2b performed well, especially in E and H, among the 11 accessed global ocean surface turbulent fluxes datasets including 6 reanalysis, 4 satellite-derived, and 1 combined. However, the assessment (Brunke et al. 2011) was mainly based on the cruise observations available during 1991-1999, while temporal positive/negative trends of the globally averaged E/WB&Qair of GSSTF2b were found increasing post 2000 that were systematically related to the negative artificial trends found in the SSM/I Tb's whose Tb19v, Tb19h, Tb22v, and Tb37v channels were used for retrieving WB, Qair, and subsequently E (Shie 2010a,b). A second dataset (Set2) of GSSTF2b was thus produced by artificially excluding certain satellite retrievals that were believed responsible for the relatively large trend occurred in the globally averaged E of Set1 mostly post 2000. Subsequently, Set2 contained a smaller global temporal trend in E post 2000 than the original dataset of GSSTF2b (i.e., renamed as Set1) did, yet for being compromised by gaining more missing data due to involving less available satellite data.

We (Hilburn and Shie 2011; Shie and Hilburn 2011) later found that the SSM/I Tb trends were mainly due to the temporal variation/drifting (decreasing) of Earth incidence angle (EIA) of the SSM/I satellites. We subsequently successfully developed a simple and accurate method for removing such EIA dependence from Tb. The detailed algorithm can be found in Hilburn and Shie (2011). An upgraded and improved GSSTF2c dataset (Shie et al. 2011; Shie 2011) using the corrected SSM/I Tb based on the developed method was thus produced. The temporal trends (% per year during 1988-2008) of the globally averaged (90°N-90°S) parameters, i.e., WB; Qair; E, were properly reduced from -0.27/-0.12; -0.20/-0.09; 1.12/0.76 in GSSTF2b-Set1/Set2 to -0.04; -0.03; 0.53 in GSSTF2c, respectively. In the GSSTF2c and GSSTF2b datasets, as aforementioned, the Qair retrieval involved applications of the WB-Tb formulation (Schulz et al. 1993) and the EOF method (Chou et al. 1995; 1997). This newly produced GSSTF3 dataset, involving an updated Qair retrieval method, i.e., using the Qair-Tb formulation in Bentamy et al. 2003, has been found further reducing the temporal trend in the retrieved Qair, and subsequently that in E. The temporal trends (% per year during 1988-2008) of the globally averaged

Qair and E have been reduced from -0.03 and 0.53 in GSSTF2c to -0.007 and 0.48 in GSSTF3, respectively. More details on the trend improvement, particularly found in Qir and E of GSSTF3 are presented as follows in the next subsection.

4.3 Quality Control and Diagnostics

As aforementioned, the temporal trends (particularly post 2000) of the globally averaged parameters, e.g., surface specific humidity, Qair, and latent heat flux, E, have subsequently reduced throughout the series of improved GSSTF datasets, i.e., from GSSTF2b-Set1, GSSTF2b-Set2, GSSTF2c to the newly produced GSSTF3. However, note that E depends on a combined effect of wind speed, U, and Qsat-Qair that may result in a more complex trend pattern than Qair. Generally, E may be reasonably considered as inversely dependent of Qair. The magnitude of the positive trend of E (i.e., 0.53/0.48 % per year during 1988-2008, for GSSTF2c/GSSTF3, respectively, as mentioned earlier) is considerably larger than that of the negative trend of Qair (i.e., -0.03/-0.007 % for GSSTF2c/GSSTF3, respectively) that is due to E's nonlinear dependence of U and Qsat-Qair, or more accurately, of U, Qair, and Qsat. Any possible positive trend occurred in U, SST (Qsat), or combined, would have played a multiplying or amplifying effect on the existing negative trend (even just a small magnitude) of Qair, and resulted in a greater positive trend for E.

Impact due to the applications of the updated Qair retrieval scheme (Bentamy et al. 2003) and the corrected SSM/I Tb on GSSTF3 is further discussed and better presented through figure (Figure 1) of the globally averaged (0-360^{o}E, 90^{o}S-90^{o}N) time series of Qair and E, respectively, from January 1988 to December 2008 (21 years), as well as figure (Figure 2) of the associated validations against ship measurements. Time series of Qair and E of GSSTF3 are shown in Figure 1a and Figure 1b, respectively, along with those of GSSTF2c, GSSTF2b-Set1 and GSSTF2b-Set2. In Figure 1a, Qair of GSSTF2c generally shows a smaller decreasing/negative trend than both GSSTF2b-Set1 & Set2, i.e., mainly due to the use of corrected Tb, while GSSTF3 shows a further reduced negative trend than GSSTF2c does, i.e., primarily due to the adoption of the updated Qair retrieval scheme. Figure 1a also clearly demonstrates that the monthly averaged Qair of GSSTF3 possesses a larger (largest) magnitude than that of its counterparts, i.e., GSSTF2b-Set1/Set2 and GSSTF2c, which leads to a positive (instead of negative) bias consistently shown in Figure 2b.

Figure 1b plainly demonstrates that the monthly averaged latent heat flux of GSSTF3 not only shows a reduced positive temporal trend than that of its counterparts, i.e., GSSTF2b-Set1/Set2 and GSSTF2c, but also possesses the smallest magnitude among all, which leads to a smaller positive bias (than GSSTF2c) consistently shown in Figure 2a. Again, the proper decrease of the positive trends in GSSTF3 and GSSTF2c are mainly due to the corrected Tb with an EIA adjustment, while the even smaller trend in GSSTF3 is attributed to the use of the updated and likely more accurate Qair-Tb relation than the WB-Tb relation.

Latent heat flux, E, and surface specific humidity, Qair, of the newly produced GSSTF3, and those of the preceding GSSTF2c, (based on the SSM/I F13) are validated against the available ship measurements from the Stratus Ocean Reference Station (20^{o}S, 85^{o}W) during 2001, 2005-2007. Figure 2a shows that GSSTF3 possesses a significantly smaller bias of E (6.27 Wm^{-2}) than that of GSSTF2c (14.96 Wm^{-2}) compared to the ship measurements. The reduced positive bias of E in GSSTF3 compared to GSSTF2c is mainly due/related to the positive bias of Qair in GSSTF3, i.e., 0.25 g kg^{-1}, compared to the negative bias of Qair in GSSTF2c, i.e., -0.25 g kg^{-1} (Figure 2b). GSSTF3, however, shows a slightly smaller correlation in both E and Qair (0.75 and 0.80) than GSSTF2c does (0.79 and 0.83). There are only 22 data pairs successfully collocated in this sample group that may not be sufficiently large enough to well represent (i.e., the associated correlations may not be significant); however, the associated biases of E and Qair are consistent to the respective features shown in Figure 1.

We have particularly performed an uncertainly analysis on the monthly-mean latent heat flux (E) and sensible heat flux (H), respectively, by including three additional peer products, i.e., HOAPS3 (Grassl et al. 2000), J-OFURO2 (Kubota et al. 2002) and OAFlux (Yu and Weller 2007), along with GSSTF3 and GSSTF2c. Note that GSSTF2c is also included with GSSTF3 in the analysis because that its Qair (thus E, particularly) retrieved based on a different algorithm shows a significant difference from that of GSSTF3 (Figure 1) even though GSSTF2c and GSSTF3 were produced using the same corrected Tb. The GSSTF2b products (Set1 or Set2) were excluded from the analysis for their using the original SSM/I Tb with questionable artificial trends. Monthly-mean fluxes (E or H) from these five products of Jan 1988-Dec 2005 (a common period with available data from all five products) have been globally averaged (80°S-80°N; 0°-360° - a maximum common domain of data availability) first since they are originally derived from various grids, i.e., GSSTF3 of 0.25° x 0.25°; HOAPS3 of 0.5° x 0.5°; GSSTF2c, J-OFURO2 and OAFlux of 1° x 1°. The mean of the globally averaged flux (E or H) from these five products is then acquired, along with the mean of the associated standard deviation, for each month of the entire time period. Throughout a temporal average (1988-2005), the overall mean and standard deviation (considered as "uncertainty") of fluxes are finally obtained, i.e., 96.64 and 3.42 Wm^{-2} for E, 9.43 and 2.65 Wm^{-2} for H, respectively. Relatively, sensible heat flux has a considerably larger percentage of uncertainty (i.e., 2.65/9.43~28.1%) than latent heat flux (i.e., 3.42/96.64~3.54%). Note that the uncertainty analysis has not been performed on the third flux component, wind stress, since wind stress is only available from GSSTF2c and GSSTF3, while they both applied the same wind fields (magnitudes or vectors) in producing wind stress. We are currently writing a peer-reviewed paper in which an extended discussion on a thorough uncertainty analysis involving additional quantities such as surface specific humidity, sea surface temperature and wind speed will be presented.

In closing this section, we would like to quote the insightful "**Rice Cooker Theory**" by Shie (2010a,b), i.e., "**To produce a bowl of delicious 'cooked rice' (useful and trustworthy 'output product') depends not only on a fine and working 'rice cooker' ('model/algorithm'), but also on good-quality 'raw rice' (genuine and reliable 'input data')**" that has further confirmed and helped us better comprehend how and why the GSSTF3 dataset of fine quality and significant improvement has been achieved – it is attributed to applications of the corrected SSM/I Tb (i.e., **good-quality 'raw rice'**) and the updated algorithm for Qair retrieval (i.e., **fine and working 'rice cooker'**).

(a)

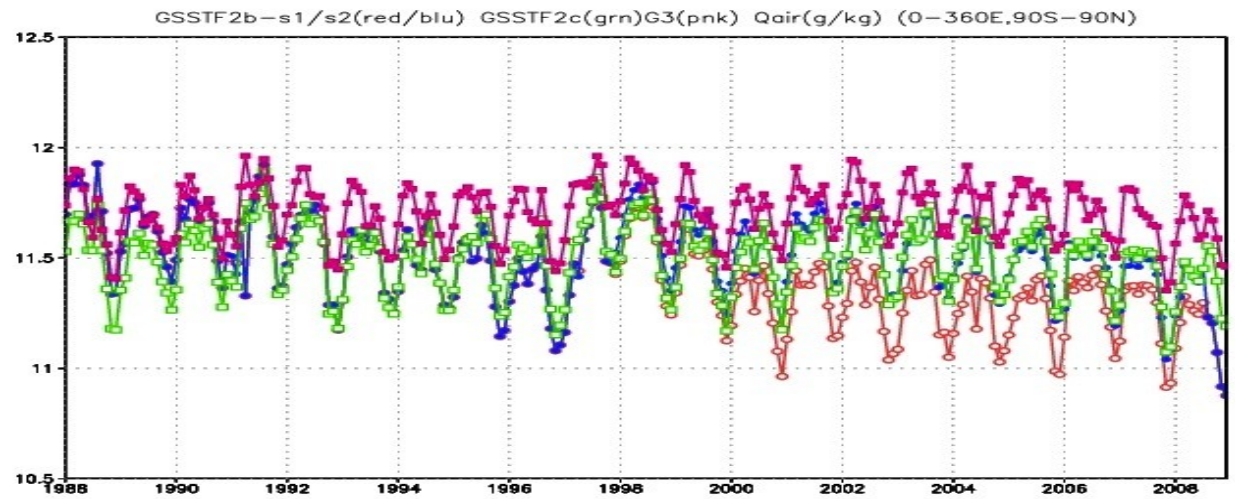

(b)

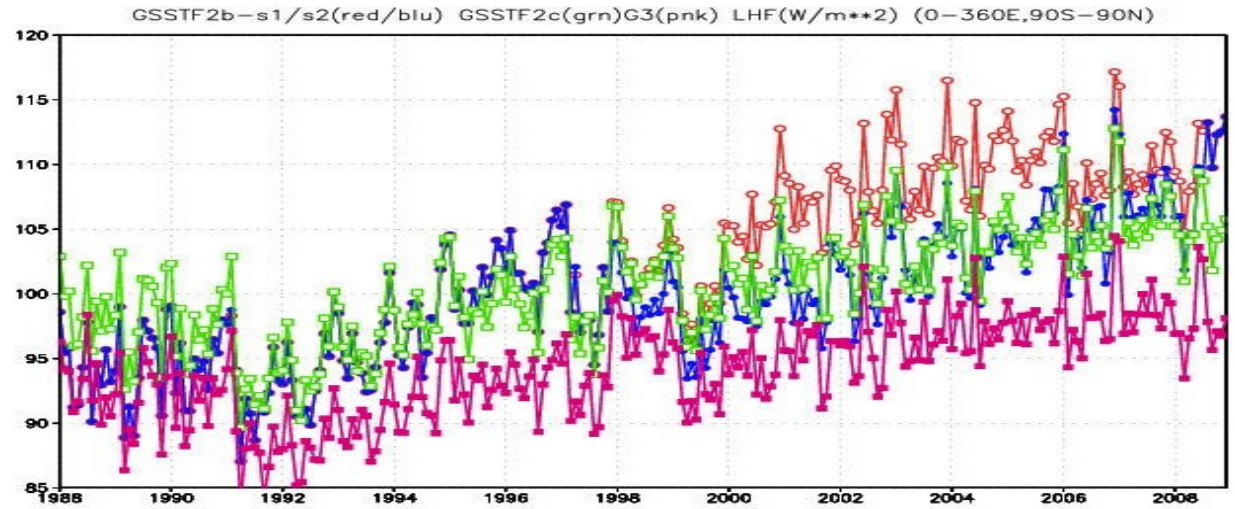

Figure 1: Global (90°N-90°S) monthly-average time series (1988-2008) of **(a)** Qair (g kg^{-1}) and **(b)** E (W m^{-2}) of GSSTF3 (pink), GSSTF2c (green), GSSTF2b-Set1 (red) and GSSTF2b-Set2 (blue).

(a)

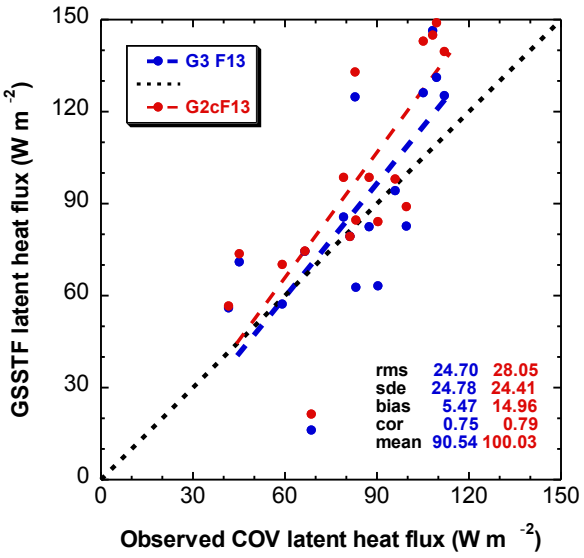

(b)

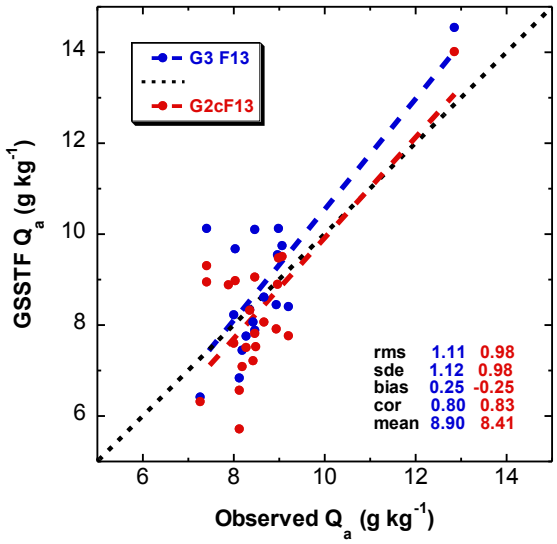

Figure 2: The GSSTF3 (based on F13) (blue) and GSSTF2c (based on F13) (red) **(a)** daily latent heat flux (W m^{-2}) and **(b)** surface specific humidity (g kg^{-1}) versus the respective measurements from the Stratus Ocean Reference Station (20S, 85W): mooring recovery and deployment cruise. There are only 22 total samples successfully collocated during 2001, 2005-2007.

4.4 Algorithm Baseline Selection

The surface specific humidity Qair is retrieved directly from the instantaneous/daily brightness temperature Tb, which is corrected by removing the EIA drifting effect (Hilburn and Shie 2011), based on the Qair-Tb relation (Bentamy et al. 2003):

$$Qair = b_0 + b_1 Tb19v + b_2 Tb19h + b_3 Tb22v + b_4 Tb37v, \quad (1)$$

where b_0, b_1, b_2, b_3, and b_4 are -55.9227, 0.4035, -0.2944, 0.3511 and -0.2395, respectively. Units of Qair and Tb are g kg^{-1} and K, respectively.

The GSSTF bulk flux model (based on the surface layer similarity theory, Chou 1993) used for performing the GSSTF3 production is essentially the same as that for GSSTF2 (Chou et al. 2003), GSSTF2b (Shie et al. 2010b; Shie 2010b), and GSSTF2c (Shie et al. 2011; Shie 2011). Similar to the preceding GSSTF datasets, GSSTF3 requires the same methodology and nearly all the same kinds of input data such as the surface/10-m wind speeds, SST, 2-m air temperature, and sea level pressure except that the "intermediate" parameters, i.e., bottom-layer precipitable water WB or total precipitable water W are no longer created or needed in GSSTF3. The air-sea turbulent fluxes, i.e., wind stress (τ), sensible heat flux (H), and latent heat flux (E) can be given in the following bulk aerodynamic formula:

$$\tau = \rho\, CD\, (U-Us)^2, \quad (2a)$$

$$H = \rho\, Cp\, CH\, (U-Us)\, (\theta s-\theta a), \quad (2b)$$

$$E = \rho\, L\upsilon\, CE\, (U-Us)\, (Qsat-Qair), \quad (2c)$$

where ρ is air density, Cp the isobaric specific heat, Lυ the latent heat of vaporization, CD, CH, CE the three respective bulk transfer coefficients, and Us is the negligibly small ocean surface current (about 0.55 of frictional velocity). The input parameters are the wind speed (U), the sea surface temperature (θs), the air potential temperature (θa), the specific humidity (Qair) at the reference height, and the saturation specific humidity (Qsat) at the sea surface temperature.

Based on surface layer similarity theory, the surface fluxes in Eqs. (2a)-(2c) can also be derived from the scaling parameters for wind or friction velocity (u_*), temperature (θ_*), and humidity (q_*) as

$$\tau = \rho\, u_*^2, \quad (3a)$$

$$H = -\rho\, Cp\, u_*\theta_*, \quad (3b)$$

$$E = -\rho\, L\upsilon\, u_* q_*. \quad (3c)$$

For a given θs (or SST) and wind, temperature, and humidity at the measurement or reference heights within the atmospheric surface layer, the scaling parameters are solved through the roughness lengths and dimensionless gradients of wind, temperature, and humidity. The dimensionless gradients of wind,

potential temperature, and humidity are functions of the stability parameter z/L, where z is the measurement height, and L the Monin–Obukhov length, which depends on the scaling parameters or fluxes (detailed description can be found in Chou et al. 2003). Accordingly, the transfer coefficients, which reflect the efficiency of the vertical transportation of momentum, heat, and moisture flux, are a non-linear function of the vertical gradient in wind speed, temperature and water vapor near the surface and, therefore, are affected by the stability of the surface air. Liu et al. (1979) performed detailed analysis of the transfer coefficients based on their model and predicted that under low wind conditions the transfer coefficient might increase with increasing wind speed, because the increased roughness facilitates the transfer of heat and vapor. However, as the wind speed increases further, the sheltering effect due to the troughs between waves becomes more significant and will suppress the exchange of vapor and heat. As the wind speed reaches about 5 m s^{-1}, the negative and positive effects due to increased wind speed counterbalance each other. If wind speed increases further, the transfer coefficient may even start to decrease. Latest field and laboratory measurements have shown that the drag coefficient does not increase with wind speed at extreme wind conditions, i.e., greater than 30 m s^{-1} (Powell et al., 2003; Donelan et al., 2004). High-wind transfer coefficients (based on Powell et al., 2003; Donelan et al., 2004; Black et al., 2007) may be applied for the 10-m winds beyond 18 m s^{-1} (or even higher) in our future/extended GSSTF production. Such a high-wind treatment may improve the surface flux retrieval, as well as provide a better understanding of weather systems with high winds such as tropical cyclones, hurricanes and typhoons.

5 Constraints, Limitations and Assumptions

Similar to the previous GSSTF products (e.g., GSSTF2c), the surface fluxes of GSSTF3 are limited to the global open-sea areas. Areas over continents/lands and the sea-ice covered oceans (i.e., high latitudes) are therefore filled with missing data.

As addressed earlier, we have updated our Qair retrieval algorithm from the previous two-step approach involving the WB-Tb relation (Schulz et al. 1993) and the EOF method (Chou et al. 1995; 1997) to the new one-step approach using the Qair-Tb relation (Bentamy et al. 2003) in the GSSTF3 production. One well-justified modification/constraint applied in the previous GSSTF EOF algorithm (Chou et al. 1997) is still retained in the updated algorithm:

In the summer, as the warmer continental (or maritime) air moves over a colder ocean surface, fog or stratus may form with the surface air reaching saturation at a temperature near the underlying cold SST. These areas are generally located over the extratropical oceans and the cold oceanic upwelling regions off the west coasts of North America, South America, and Africa during the summer. Under this situation the specific humidity in the lower atmosphere may either increase with height or decrease less rapidly, namely, the surface specific humidity may be lower (or lowest) or not considerably higher than its ambient environment above. As such, the algorithm (e.g., Chou et al. 1995) tends to overestimate the

surface humidity when fog or stratus forms. To reduce the likely overestimated surface humidity under such situation using this updated algorithm, the saturation specific humidity (Qsat) of daily SSTs is also used as an upper bound for the retrieval of SSM/I surface humidity.

In closing, we would like to reiterate the importance of acquiring/using quality input datasets in the GSSTF flux production that is elaborated earlier via the quotation of the "Rice Cooker Theory". The recently improved SSM/I Tb, incorporating proper adjustments to the drifts in the Earth Incidence angle (EIA), has genuinely improved the quality of the retrieved Qair and E of GSSTF3 and those of the preceding GSSTF2c. So does the adoption of the updated Qair retrieval algorithm further improve the quality of Qair and E of GSSTF3. Moreover, as previously mentioned in Shie 2011, authenticity of the input NCEP SST and Tair_2m improve the quality of the retrieved H. Nonetheless, there should always be a room for us to further improve our future GSSTF flux product by acquiring further genuine and more reliable input datasets/parameters, as well as seeking a continual improvement/development in our GSSTF model/scheme.

6 Acknowledgement

This author C.-L. Shie, also the principal investigator (PI) of this revived GSSTF project, wishes to dedicate this GSSTF3 product, again to his mentor: the late research scientist S.-H. Chou (aka Sue). Without her genuine intelligence and intuition, great vision and perseverance, the productions of the newly upgraded GSSTF3 and the preceding GSSTF2c, GSSTF2b would have not been possible. The PI sincerely wishes to thank his collaborators R. Adler, J. Ardizzone, S. Braun, L. Chiu, S. Gao, I. Lin, E. Nelkin and F.-C. Wang for their crucial contributions and supports of this GSSTF project, while a special thanks goes to K. Hilburn for his crucial contribution of successfully developing a useful algorithm properly resolving the SSM/I Tb trends due to the drifts of EIA. The PI also owes a special thanks to A. Savtchenko for his precious help and great efforts in converting the GSSTF datasets from the original binary format into the HDF-EOS5 format for the official distributions via NASA GES DISC. A special thanks also goes to B. Vollmer, D. Ostrenga, S. Kempler and G. Hunolt for their precious helps in the official distributions of GSSTF3 (and GSSTF2c, GSSTF2b previously); and J. Moses for his precious help in the new installation of DOI into the GSSTF3 data products.

This study is supported by the MEaSUREs Program of NASA Science Mission Directorate-Earth Science Division. The PI is especially grateful to its Program Manger M. Maiden, Assistant Program Manager H. K. Ramapriyan, and Program Scientist J. Entin for their invaluable and persistent supports of this research.

7 References

Atlas R. M., J.V. Ardizzone, R. N. Hoffman, and J. C. Jusem, 2009: The cross-calibrated, multi-platform (CCMP) ocean surface wind product: Current status and plans. *The 2009 AGU Fall Meeting*, San Francisco, CA, December 14-18, 2009.

Bentamy A., K B. Katsaros, M. Alberto, W. M. Drennan, E. B. Forde, and H. Roquet, 2003: Satellite Estimates of wind speed and latent heat flux over the global oceans, *J. Climate*, **16**, 637-656.

Black, P. G., E. A. D'Asaro, W. M. Drennan, J. R. French, P. P. Niiler, T. B. Sanford, E. J. Terrill, E. J. Walsh, and J. A. Zhang, 2007: Air-sea exchanges in hurricanes. *Bull. Amer. Meteor. Soc.*, **88**, 357-374.

Chou, S.-H., 1993: A comparison of airborne eddy correlation and bulk aerodynamic methods for ocean-air turbulent fluxes during cold-air outbreaks. *Bound.-Layer Meteor.*, **64**, 75-100.

Chou, S.-H., R. M. Atlas, C-L. Shie and J. Ardizzone, 1995: Estimates of surface humidity and latent heat fluxes over oceans from SSM/I data, *Monthly Weather Review,* **123**, 2405-2425.

Chou, S.-H., C.-L. Shie, R. M. Atlas, and J. Ardizzone, 1997: Air-sea Fluxes Retrieved from Special Sensor Microwave Imager Data, *Journal of Geophysical Research*, **102**, 12705-12726.

Chou, S.-H., E. Nelkin, J. Ardizzone, R. Atlas, and C.-L. Shie, 2001: The Goddard Satellite-Based Surface Turbulent Fluxes Dataset --- Version 2 (GSSTF 2.0) [global (grid of 1°x1°) daily air-sea surface fluxes from July 1987 to December 2000] distributed by Goddard DISC at http://disc.sci.gsfc.nasa.gov/precipitation/data-holdings/access/gsstf2.0.shtml/.

Chou, S.-H., E. Nelkin, J. Ardizzone, R. M. Atlas, and C.-L. Shie, 2003: Surface turbulent heat and momentum fluxes over global oceans based on the Goddard satellite retrieval, version 2 (GSSTF2). *J. Climate*, **16**, 3256-3273.

Donelan M. A., B. K. Haus, N. Reul, W. J. Plant, M. Stiassnie, H. C. Graber, O. B. Brown, and E. S. Saltzman, 2004: On the limiting aerodynamic roughness of the ocean in very strong winds, *Geophys. Res. Lett.*, **31**, L18306.

Grassl, H., V. Jost, M. R. Ramesh Kumar, J. Schulz, B. Bauer, and P. Schluessel, 2000: The Hamburg Ocean Atmosphere Parameters and Fluxes from Satellite data (HOAPS): a climatological Atlas of satellite derived air–sea interaction parameters over the oceans. *Max Planck Report*, No. 312, 130 pp.

Hilburn, K. A. and C.-L. Shie, 2011: Decadal trends and variability in Special Sensor Microwave Imager (SSM/I) brightness temperatures and Earth incidence angle. Report No. 092811, Remote Sensing Systems, 53 pp. (Available online at: http://www.remss.com/papers/tech_reports/hilburn_SSMI_EIA_TB_RSS_Tech_Rpt_092811.pdf)

Kubota, M., K. Ichikawa, N. Iwasaka, S. Kizu, M. Konda, and K. Kutsuwada, 2002: Japanese Ocean Flux Data Sets with Use of Remote Sensing Observations (J-OFURO). *J. Oceanogr.*, **58**, 213–215.

Liu W. T., K. B. Katsaros, and J. A. Businger, 1979: Bulk parameterization of air-sea exchanges of heat and water vapor including the molecular constraints at the interface. *J. Atmos. Sci.*, **36**, 1722–1735.

Powell, M. D. P. J. Vickery, and T. A. Reinhold, 2003: Reduced drag coefficient for high wind speeds in tropical cyclones, *NATURE*, **422**, 279-283.

Schulz J., P. Schluessel, and H. Grassl, 1993: Water vapor in the atmospheric boundary layer over oceans from SSM/I measurements. Int. J. Remote Sens., **14**, 2773–2789.

Schulz, J., J. Meywerk, S. Ewald, and P. Schluessel, 1997: Evaluation of satellite-derived latent heat fluxes. *J. Climate*, **10**, 2782–2795.

Shie, C.-L., L. S. Chiu, R. Adler, E. Nelkin, I-I Lin, P. Xie, F.-C. Wang, R. Chokngamwong, W. Olson, and D. A. Chu, 2009: A note on reviving the Goddard Satellite-Based Surface Turbulent Fluxes (GSSTF) dataset. *Adv. Atmos. Sci.*, **26**, No. 6, 1071-1080. Available from ftp://meso-a.gsfc.nasa.gov/pub/shieftp/fluxdocu/gsstf2b/Shie-et-al-AAS2009.pdf

Shie, C.-L., 2010a: A recently revived dataset of satellite-based global air-sea surface turbulent fluxes (GSSTF2b) – features and applications. *The 17th Conf. on Sat. Meteor. and Oceanog.*, 27 September – 1 October 2010, Annapolis, MD. (Keynote speech) Available from ftp://meso-a.gsfc.nasa.gov/pub/shieftp/fluxdocu/gsstf2b/2010_Sat_Air_Sea-Shie.pdf

Shie, C.-L., 2010b: Science background for the reprocessing and Goddard Satellite-based Surface Turbulent Fluxes (GSSTF2b) Data Set for Global Water and Energy Cycle Research, In: *NASA GES DISC*, 18 pp, October 12, 2010. Available from ftp://meso-a.gsfc.nasa.gov/pub/shieftp/fluxdocu/gsstf2b/Science_of_the_data.GSSTF2b.pdf

Shie, C.-L., L. S. Chiu, R. Adler, S. Gao, R. Chokngamwong, I-I Lin, E. Nelkin, J. Ardizzone, P. Xie, and F.-C. Wang, 2010a: A recently revived and produced global air-sea surface turbulent fluxes dataset – GSSTF2b: Validations and Findings. *Proceedings of the Joint 2010 CWB Weather Analysis and Forecasting & COAA 5th International Ocean-Atmosphere Conference*, 307-312, Taipei, Taiwan, June 28-30, 2010.

Shie, C.-L., L. S. Chiu, R. Adler, I-I Lin, E. Nelkin, and J. Ardizzone, 2010b: The Goddard Satellite-Based Surface Turbulent Fluxes Dataset --- Version 2b (GSSTF2b), In: *NASA Goddard Earth Sciences (GES) Data and Information Services Center (DISC)*, October 2010. (retired in June 2012)

Shie, C.-L., 2011: Science background for the reprocessing and Goddard Satellite-based Surface Turbulent Fluxes (GSSTF2c) Data Set for Global Water and Energy Cycle Research. *Science Document for the Distributed GSSTF2c via Goddard Earth Sciences (GES) Data and Information Services Center (DISC)*, 19 pp. Available from http://disc.sci.gsfc.nasa.gov/measures/documentation/Science_of_the_data.GSSTF2c.pdf or ftp://meso-a.gsfc.nasa.gov/pub/shieftp/fluxdocu/gsstf2c/Science_of_the_data.GSSTF2c.pdf

Shie, C.-L. and K. Hilburn, 2011: A satellite-based global ocean surface turbulent fluxes dataset and the impact of the associated SSM/I brightness temperature, *Proceedings of The 2011 EUMETSAT Meteorological Satellite Conference*, Oslo, Norway, September 5-9, 2011, 8 pp. Available from ftp://meso-a.gsfc.nasa.gov/pub/shieftp/fluxdocu/gsstf2c/Shie&Hilburn-2011.pdf

Shie, C.-L., K. Hilburn, L. S. Chiu, R. Adler, I-I Lin, E. Nelkin, and J. Ardizzone, 2011: The Goddard Satellite-Based Surface Turbulent Fluxes Dataset --- Version 2c (GSSTF2c), In: *NASA Goddard Earth Sciences (GES) Data and Information Services Center (DISC)*, October 2011, Available from ftp://aurapar1u.ecs.nasa.gov/data/s4pa/GSSTF/ or http://disc.sci.gsfc.nasa.gov/daac-bin/DataHoldingsMEASURES.pl?PROGRAM_List=ChungLinShie

Woodruff, S. D., S. J. Lubker, K. Wolter, S. J. Worley, and J. D. Elm, 1993: Comprehensive Ocean-Atmosphere Data Set (COADS) release la: 1980–92. *Earth System Monitor*, **4**, 4–8.

Xing, Y., 2006: Recent changes in oceanic latent heat flux from remote sensing, Ph.D. Dissertation, School of Computational Science, George Mason University, Fairfax VA 22030, 119 pp.

Yu, L., and R. A. Weller, 2007: Objectively Analyzed Air-Sea Heat Fluxes for the global ice-free oceans (1981-2005). *Bull. Amer. Meteorol. Soc.*, **88**, 527-539.